JOURNAL OF VIROLOGY, May 1991, p. 2372–2380
0022-538X/91/052372-09$02.00/0
Copyright © 1991, American Society for Microbiology
Vol. 65, No. 5

Myristoylation Is Important at Multiple Stages in Poliovirus Assembly

NICOLA MOSCUFO,[1] JOHN SIMONS,[2] AND MARIE CHOW[1]*

Departments of Biology[1] and Applied Biological Sciences,[2] Massachusetts Institute of Technology, Cambridge, Massachusetts 02139

Received 1 November 1990/Accepted 28 January 1991

The N-terminal glycine of the VP4 capsid subunit of poliovirus is covalently modified with myristic acid (C_{14} saturated fatty acid). To investigate the function of VP4 myristoylation in poliovirus replication, amino acid substitutions were placed within the myristoylation consensus sequence at the alanine residue (4003A) adjacent to the N-terminal glycine by using site-directed mutagenesis methods. Mutants which replace the alanine residue with a small hydrophobic residue such as leucine, valine, or glycine displayed normal levels of myristoylation and normal growth kinetics. Replacement with the polar amino acid histidine (4003A.H) also resulted in a level of myristoylation comparable to that of the wild type. However, replacement of the alanine residue with aspartic acid (4003A.D) caused a dramatic reduction (about 40 to 60%) in myristoylation levels of the VP4 precursors (P1 and VP0). In contrast, no differences in modification levels were found in either VP0 and VP4 proteins isolated from mature mutant virions, indicating that myristoylation is required for assembly of the infectious virion. The myristoylation levels of the VP0 proteins found in capsid assembly intermediates indicate that there is a strong but not absolute preference for myristoyl-modified subunits during pentamer formation. Complete myristoylation was observed in mature virions but not in assembly intermediates, indicating that there is a selection for myristoyl-modified subunits during stable RNA encapsidation to form the mature virus particle. In addition, even though mutant infectious virions are fully modified, the severe reduction in specific infectivity of both 4003A.D and 4003A.H purified viruses indicates that the amino acid residue adjacent to the N-terminal glycine apparently has an additional role early during viral infection and that mutations at this position induce pleiotropic effects.

Poliovirus is a positive-strand RNA virus whose genome is enclosed in an icosahedrally symmetric shell formed by 60 copies of each of the capsid subunits VP1, VP2, VP3, and VP4 (15). VP4 subunits are modified at the N-terminal glycine residue with myristate (C_{14} saturated fatty acid) (9). Crystallographic analysis of the virion structure revealed the location of this fatty acid and displayed its extensive involvement in subunit-subunit interactions within this multimeric protein complex. This suggested that myristoyl modification may be important during capsid assembly. Viral mutants lacking myristoylation are nonviable and fail to make viral capsids (22, 23, 32). However, assembly intermediates have been identified in mutant transfected cells (23). Other in vitro studies have suggested that myristoylation is necessary for correct proteolytic processing of the capsid protein precursors (18, 22). To date there is no direct evidence identifying the critical roles of this modification during poliovirus infection.

One experimental strategy is to alter the myristoylation signal sequence. In particular, the identity of the amino acid residue adjacent to the N-terminal glycine appears to affect the modification kinetics of the yeast N-myristoyl transferase (NMT) in vitro (35–37). The data presented here demonstrate that normal levels of myristoylation are observed in poliovirus mutants in which the wild-type alanine residue is replaced with leucine, valine, glycine, or histidine. Replacement of the alanine with an aspartic acid results in down-modulation of the myristoylation process in vivo, leading to partial myristoyl modification of the capsid proteins. In vivo characterization of this viral mutant demonstrates that partial myristoylation does not appear to affect proteolytic processing of the capsid or other nonstructural proteins. Significantly, there is a kinetic preference for myristoylated proteins during formation of the pentamer intermediate in the capsid assembly pathway and a strong requirement for myristoylation during RNA encapsidation and formation of the mature virus particle.

* Corresponding author.

MATERIALS AND METHODS

Cells. HeLa cells were grown in suspension in Joklik's modified minimal essential medium (Hazelton) supplemented with 5% horse serum (GIBCO). HeLa cell monolayers were maintained in Dulbecco's modified medium supplemented with 5% fetal calf serum (FCS). All virus dilutions were performed in phosphate-buffered saline (PBS).

Bacterial strains and plasmids. Phage stocks, phage replicative-form DNA, and all plasmids were grown in *Escherichia coli* XL-1 Blue (Stratagene Cloning Systems). *E. coli* CJ236 was used to generate phage stocks containing uridylated genomes. Plasmid DNAs were isolated from the bacteria and purified on CsCl gradients (3). Plasmid pPVM1, containing an infectious cDNA copy of the poliovirus genome (serotype 1, Mahoney strain), was originally obtained from P. Sarnow (University of Colorado Medical School, Denver).

Nomenclature. The site of a mutation is identified with a four-digit code. The first digit indicates the poliovirus capsid subunit, and the last three digits refer to the amino acid position within that capsid protein. The number is followed by the single-letter code for the amino acid present in the wild-type parent strain. For VP4, residue 1 is the initiating methionine (4001M), which is removed within the infected

cell by a cellular methionyl peptidase. The N-terminal glycine residue is designated 4002G. Mutants are indicated by an additional single-letter code for the new residue. For example, 4003A.D indicates that an aspartic acid replaces the wild-type alanine at amino acid residue 3 of VP4. To be consistent with the nomenclature used for other poliovirus mutants (2), the full name of 4003A.D is IC-VP4003A.D.

4003 mutant constructions. Sequences encoding the 5′ coding region of the poliovirus genome (from nucleotides 1 to 1641, Mahoney strain) were subcloned into M13mp19. Synthetic deoxyoligonucleotides, corresponding to the region of the poliovirus genome between nucleotides 739 and 759, were synthesized with a random mixture of nucleotides at positions 749, 750, and 751 (Massachusetts Institute of Technology biopolymer facility), thus allowing for a variety of amino acid substitutions to occur at amino acid 3 of the VP4 capsid region. The synthetic oligonucleotides were incorporated by the method of Kunkel (20). Amino acid substitutions were identified by dideoxynucleotide sequence analysis of individually recovered phage genomes (29). For specific amino acids of interest, full-length poliovirus genomic cDNAs were generated by replacing the 1.2-kb *Sfi*I-*Aat*II wild-type fragment in the pPVM1 plasmid with the identical fragment from the mutant subclone. The sequence of the constructed full-length mutant viral cDNA was determined to confirm the identities and locations of the amino acid substitutions (29). Sequences of viable mutant viruses were determined by direct sequence analysis of the RNA genome using avian myeloblastosis virus reverse transcriptase (Life Sciences Inc.) (24).

DNA transfection. HeLa cell monolayers (70 to 80% confluent) in 10-cm-diameter plates were transfected with DEAE-dextran and 1 μg of pPVM1 (33). After incubation for 30 min at room temperature, the cells were incubated for 4 h at 37°C in Dulbecco's modified medium containing 10% FCS. The medium was replaced with 20 ml of Dulbecco's modified medium–10% FCS–1% agarose, and monolayers were incubated for 4 days at 37 or 33°C. Plaques were visualized with 1% crystal violet.

Propagation of virus stocks. Well-isolated plaques were picked from the agar overlay and placed in 1 ml of PBS. Each plaque was amplified by infecting confluent HeLa cell monolayers (10^7 cells) in 10-cm-diameter plates at low multiplicities of infection (MOI of 0.01 to 0.1). Virus-containing medium was collected 2 days later; titers of the supernatants were determined, and the supernatants were stored at −20°C. These low-MOI stocks were used to infect cells at high multiplicities for all biochemical experiments. To isolate purified virus, HeLa cells (4×10^8) were infected in suspension at an MOI of 10 and incubated at 37°C. At 6 h postinfection (p.i.), infected cells were harvested. The cell pellet was subjected to three cycles of freeze-thaw and subsequently lysed in 10 mM Tris-HCl (pH 7.5)–10 mM NaCl–1.5 mM $MgCl_2$–1% Nonidet P-40 (5×10^7 cells per ml). After removal of the nuclei by centrifugation, virus in cell lysate was purified by CsCl density gradients (28). Purified virus was equilibrated in TNE (50 mM Tris [pH 7.5], 100 mM NaCl, 0.1 mM EDTA) and stored at −20°C.

Single-cycle growth curves. Suspended HeLa cells (2×10^7) were infected with mutant or wild-type virus at high multiplicities (MOI of 10). After incubation at room temperature for 30 min, the cells were washed twice with PBS, suspended in 5 ml of minimal essential medium–5% FCS, and incubated at 37°C. At various times p.i., 100-μl aliquots were removed. The virus was released from the cells by multiple cycles of freeze-thaw, and the infectious titer in each sample was determined by plaque assays (8).

Labeling of infected cells. Labeled cell lysates were made from infected HeLa cells grown in either monolayer or suspension culture. HeLa cells in suspension (4×10^7 cells) or in confluent monolayers (10^7 cells) were washed twice with PBS and infected with wild-type or mutant viruses (MOI of 10). After 30 min at room temperature, the cells were washed with PBS and incubated at 37°C in methionine-free medium supplemented with 5% FCS and 1% dimethyl sulfoxide. Dactinomycin (5 μg/ml) was added 15 min p.i. Infected HeLa cell monolayers were labeled at 3 h p.i. with [^{3}H]myristate (40 μCi/ml, 40 Ci/mmol; NEN Dupont) alone or in combination with [^{35}S]methionine (1 μCi/ml, 2 Ci/mmol; NEN Dupont). HeLa cell suspension cultures were labeled at 3 h p.i. with [^{3}H]myristate (100 μCi/ml, final concentration; 40 Ci/mmol) and [^{35}S]methionine (25 μCi/ml, final concentration; 500 Ci/mmol). Cells were harvested and washed with PBS.

Whole-cell lysates. Infected HeLa cell monolayers were lysed in RIPA buffer (10 mM Tris-HCl [pH 7.5], 150 mM NaCl, 1% deoxycholate, 1% Triton X-100, 0.1% sodium dodecyl sulfate [SDS]) at 2×10^7 cells per ml. Nuclei were removed by centrifugation, and the cell extracts were further clarified at 80,000 × *g* for 30 min at 4°C. Samples to be analyzed by SDS-gel electrophoresis were precipitated in 90% acetone (vol/vol) for 1 h at −20°C. The protein pellet was suspended in solubilizing buffer (62 mM Tris-Cl [pH 6.8], 5% SDS) and subjected to electrophoresis through 10 or 13% SDS-polyacrylamide gels (21). Gels were soaked in Enlighting (NEN Dupont), dried, and fluorographed at −70°C.

Analysis of assembly intermediates by sucrose gradient. Poliovirus assembly intermediates were isolated from radiolabeled HeLa cell suspension cultures infected with the high-MOI-generated virus stocks. Cells were lysed in TNM (10 mM Tris-HCl [pH 7.5], 10 mM NaCl, 1.5 mM $MgCl_2$, 1% sodium deoxycholate, 1% Brij 58, 0.05 mM phenylmethyl sulfonyl fluoride; final concentration, 3×10^7 cells per ml) at 4°C for 20 min (12). Lysates were centrifuged at 900 × *g* for 10 min at 4°C to pellet the nuclei, and equal volumes of supernatants were layered onto 6 to 25% and 10 to 30% linear sucrose gradients in TNM. Protomer and pentamer subunits were isolated from 6 to 25% sucrose gradients after centrifugation at 4°C in an SW40 rotor at 40,000 rpm for 16.5 h. Empty capsids and mature virus were isolated from 10 to 30% gradients after centrifugation at 4°C in an SW27.1 rotor at 26,000 rpm for 4 h. Gradients were fractionated and counted. Peak fractions at desired sedimentation values were pooled, dialyzed in TNM, and subjected to SDS-polyacrylamide gel electrophoresis as described above.

Quantitation of myristate modification. Radiolabeled protein bands were identified from the fluorograph and excised from the SDS-polyacrylamide gel. The gel slice was incubated overnight with 1 ml of NCS tissue solubilizer (Amersham) at 37°C. Hydrofluor scintillation liquid was added, and ^{3}H and ^{35}S counts were determined. After subtraction of the background, counts were corrected for differential counting efficiency of the two isotopes and spillover between the counting channels.

RESULTS

To identify the biological roles of myristoylation in poliovirus replication, the myristoyl recognition sequence was mutated at alanine VP4 amino acid residue 3 (4003A), the

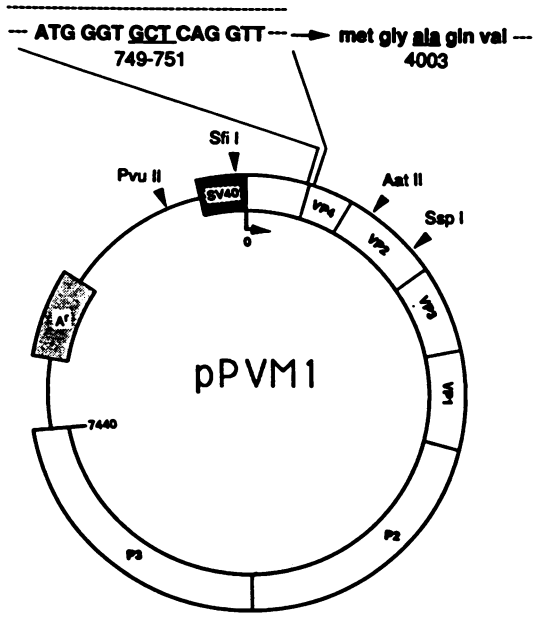

FIG. 1. Poliovirus expression vector (pPVM1) used to generate 4003 mutants. Transcription of the infectious cDNA sequence of the poliovirus genome (serotype 1, Mahoney strain) initiates from the simian virus 40 early promoter (SV40). Regions encoding each of the capsid protein subunits (VP4, VP2, VP3, and VP1) and the nonstructural protein precursors (P2 and P3) are shown. Arrows indicate the restriction sites used during vector manipulation. The nucleotide and amino acid sequences of the N-terminal region of VP4 are shown with the alanine codon targeted by the site-directed mutagenesis procedure underlined. The vector also carries the β-lactamase gene (A^r).

residue adjacent to the N-terminal glycine (Fig. 1). Amino acid differences at this position in synthetic hexa- and octapeptide substrates were shown previously to affect the kinetics in vitro of the yeast NMT (35, 37), whose substrate specificity appears to largely overlap with the murine NMTs (36). Thus, by analogy, substitutions at 4003A were likely to affect the kinetics in vivo of the human NMT.

All 4003A mutations that were reconstructed into the full-length infectious clone, except for the arginine substitution, generated viable viral mutants upon transfection into HeLa cell monolayers (Fig. 2). This is in contrast to the nonviability of all 4002G mutants constructed (22, 32). No temperature or host range differences were observed (data not shown). The wild-type-like plaque phenotypes of 4003A.G, 4003A.L, and 4003A.V indicated that the glycine, leucine, and valine substitutions did not substantially affect overall viral replication. However, substitutions with charged amino acids generated a nonviable mutant (4003A.R) or viable mutants with small-plaque (4003A.H) or microplaque (4003A.D) phenotypes.

The effects of these 4003A substitutions on myristoyl modification were examined for all viable mutant constructs. The poliovirus RNA genome encodes a single large translational product (220 kDa) from which the capsid protein precursor (P1) and nonstructural protein precursors (P2 and P3) are derived by proteolytic cleavages (19). P1 (97 kDa) is processed by viral protease 3CD to VP0 (37 kDa), VP3 (26 kDa), and VP1 (34 kDa) (39). VP0 cleavage to VP4 (7 kDa) and VP2 (31 kDa) is associated with RNA encapsidation and formation of the mature particle (28). Consistent with myristoylation of other cellular and viral proteins (11, 38), the N terminus of P1 is modified cotranslationally with myristate (13; unpublished data); all N-terminus-containing products of P1, namely VP0 and VP4, are myristoyl modified (9). In addition, poliovirus shuts off host protein synthesis. Thus,

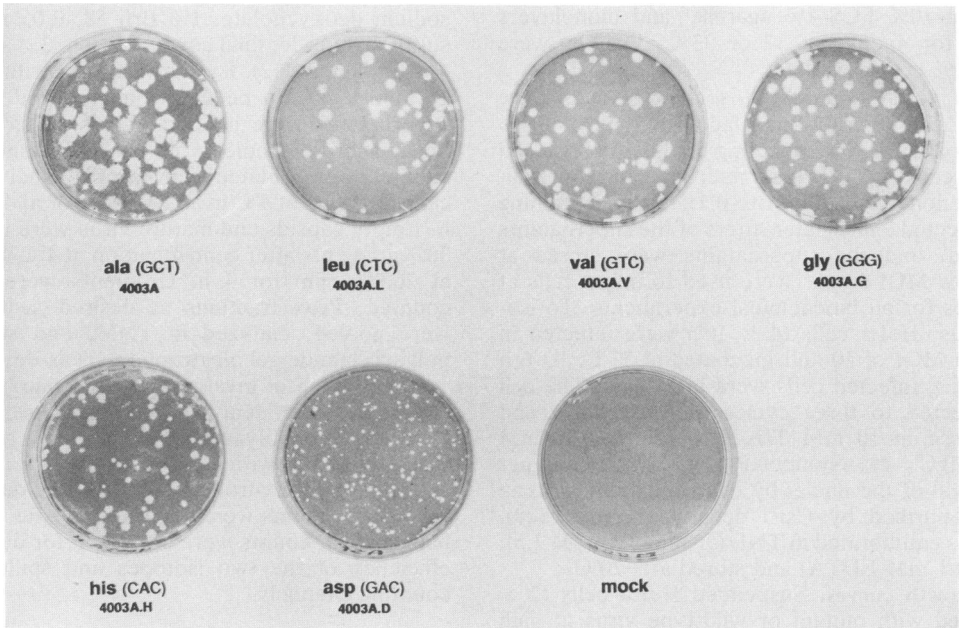

FIG. 2. Plaque phenotypes of viable poliovirus 4003 mutants. HeLa cells were infected with transfection-derived plaque isolates of mutant or wild-type viruses. Monolayers were incubated for 3 days at 37°C and stained with crystal violet. The amino acid substitution and its codon (in parentheses) are shown. Thus the alanine residue in the wild-type virus (4003A) was replaced with a leucine (4003A.L), valine (4003A.V), glycine (4003A.G), histidine (4003A.H), or aspartic acid (4003A.D) residue. The identity of the amino acid substitution was confirmed by RNA sequence analysis of mutant viral genomes.

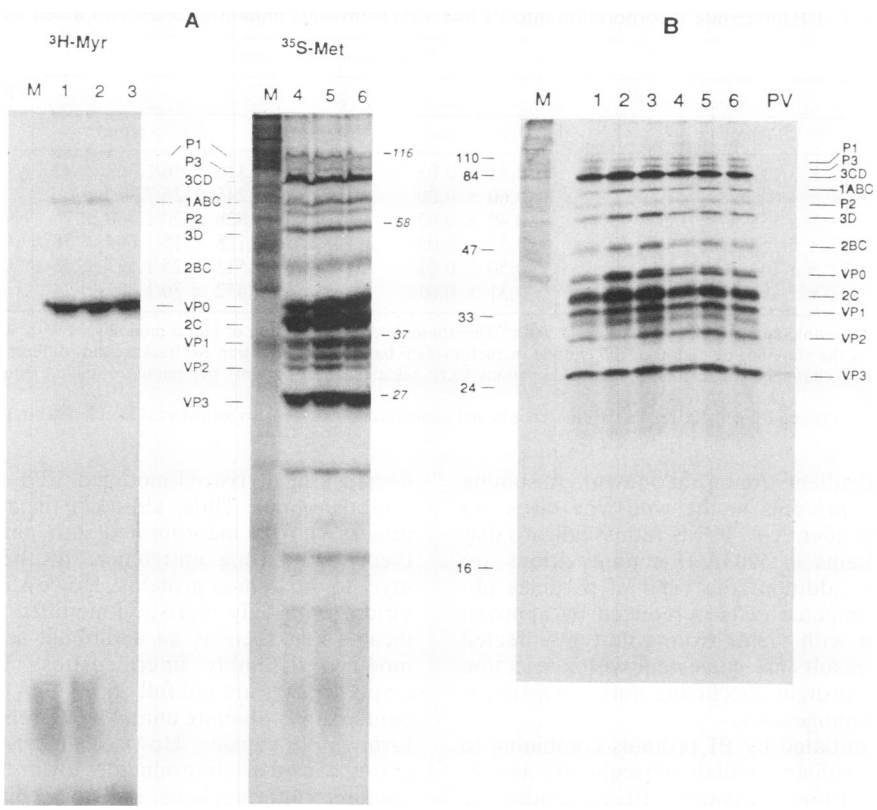

FIG. 3. [^{3}H]myristate and [^{35}S]methionine labeling of 4003 mutant-infected cells. (A) HeLa cells in monolayer were infected with wild type (lanes 1 and 4), 4003A.H (lanes 2 and 5), or 4003A.D (lanes 3 and 6). Mock (M)- or virus-infected cells were continuously labeled from 3 to 6 h p.i. with [^{3}H]myristate (lanes 1 to 3) and [^{35}S]methionine (lanes 4 to 6). Lysates were separated on 13% SDS-polyacrylamide gels. Molecular mass markers (in kilodaltons) and labeled viral proteins are indicated. (B) Infected HeLa cell monolayers were labeled from 3 to 6 h p.i. with [^{35}S]methionine (20 μCi/ml, 1,130 Ci/mmol). Lysates were from mock-infected cells (lane M) or from cells infected with wild type (lane 1), 4003A.D (lane 2), 4003A.H (lane 3), 4003A.L (lane 4), 4003A.V (lane 5), or 4003A.G (lane 6) and were separated on a 13% acrylamide gel. Purified wild-type virus virions (lane PV) served as markers. Migrations of molecular mass markers (left; in kilodaltons) and viral proteins (right) are indicated.

myristoyl modification of the VP4 capsid precursor proteins, VP0 and P1, can be qualitatively assessed by metabolic labeling of the viral proteins with [^{3}H]myristate in the absence of host protein synthesis (Fig. 3A). Myristoylation levels in 4003A mutants relative to that observed in wild type were quantitated in lysates obtained from infected cells double labeled with both [^{3}H]myristate and [^{35}S]methionine. Infected cell lysates were separated on SDS-polyacrylamide gels, and the P1 and VP0 protein bands were excised and counted. Measurement of the ^{3}H/^{35}S ratios for P1 and VP0 proteins allowed normalization for potential differences in protein synthesis and preferential processing by the different mutants. The ^{3}H/^{35}S ratios obtained for P1 and VP0 proteins from 4003A.G-, 4003A.L-, and 4003A.V-infected cell lysates were identical to those observed in wild-type (4003A)-infected cell lysates (Table 1). Thus, myristoyl modification occurs at normal levels in these mutants. Reduced VP0 modification levels in 4003A.H-infected cell lysates were occasionally observed. However, this reduction was inconsistent between different experiments, and modification levels of P1 always appeared normal. Thus this reduction in VP0 modification levels for the 4003A.H mutant is probably due to experimental variability. Myristoylation levels in P1 protein are significantly reduced in 4003A.D mutant-infected cell lysates (Fig. 3A, lane 3). Quantitation of this reduction indicated that myristoylation is reduced in 4003A.D-infected cells to approximately 60% of normal (Table 1). Interestingly, the relative reduction was similar in P1 and VP0. Additionally, the distribution of [^{35}S]methionine counts within all major viral protein compartments (P1, P2, P3, 3CD, 2B, 2C, VP1, and VP3) was identical in 4003A (wild-type)- and 4003A.D-infected cells (data not shown). Thus, overall proteolytic processing of the P1 protein to VP0-VP3-VP1 in vivo by the 3CD viral protease appears unaffected, and no strong selection for myristoylated P1 appears to exist during processing. Greater amounts of VP0 together with reduced levels of VP2 were observed consistently in 4003A.D-infected cells (Fig. 3B, lane 2). This is due to the slower rate of virus particle maturation, which leads to an apparent accumulation of VP0 in the whole-cell lysate (see below).

Reduced ^{3}H/^{35}S ratios of P1 and VP0 indicate that there are two populations of these proteins (myristoylated and nonmyristoylated) present at approximately equal concentrations in 4003A.D-infected cells. Virus, double labeled with [^{3}H]myristate and [^{35}S]methionine, was purified by sucrose sedimentation, and ^{3}H/^{35}S ratios were determined to examine whether the VP4 and VP0 proteins present in 4003A.D virion particles were also partially modified with myristate (Table 2). No difference in ^{3}H/^{35}S ratios for VP0 or VP4 was observed between wild-type and 4003A.D mutant virions. Similar results were obtained when virus was puri-

TABLE 1. [^{3}H]myristate incorporation into P1 and VP0 from 4003 mutant-infected HeLa cell extracts[a]

Mutant	[^{3}H]myristate incorporation in:			
	P1		VP0	
	^{3}H/^{35}S (cpm)[b]	^{3}H/^{35}S ratio[c]	^{3}H/^{35}S (cpm)	^{3}H/^{35}S ratio
4003A	60 ± 3/119 ± 14	0.51 ± 0.03	2,316 ± 56/1,368 ± 42	1.69 ± 0.07
4003A.L	38 ± 4/64 ± 3	0.60 ± 0.09	1,246 ± 26/724 ± 13	1.72 ± 0.07
4003A.V	75 ± 8/155 ± 9	0.49 ± 0.02	1,828 ± 20/1,106 ± 7	1.65 ± 0.03
4003A.G	92 ± 5/168 ± 1	0.55 ± 0.03	2,728 ± 15/1,604 ± 38	1.70 ± 0.05
4003A.H	72 ± 1/144 ± 4	0.50 ± 0.01	2,513 ± 25/1,677 ± 35	1.50 ± 0.02
4003A.D	27 ± 2/89 ± 1	0.31 ± 0.01	1,472 ± 30/1,302 ± 24	1.13 ± 0.04

[a] Proteins P1 and VP0 were double labeled with [^{3}H]myristate and [^{35}S]methionine during infection of HeLa monolayers with 4003 mutants.
[b] Each value is the mean ± the standard deviation of the isotope in each protein band after correction for background, differential counting efficiency, and spillover between the counting channels. Means and standard deviations were calculated from counts per minute obtained from several (more than three) determinations of 10 min each.
[c] Differences in ^{3}H/^{35}S ratios between P1 and VP0 reflect the difference in methionine content for the two proteins (24 methionines in P1 and 7 methionines in VP0).

fied by CsCl density gradients (data not shown). Assuming that all VP4 and VP0 proteins in the wild-type virus are myristoyl modified, the identical ^{3}H/^{35}S ratios indicate that all VP4 and VP0 proteins in 4003A.D mutant virions are myristoyl modified. In addition, the yield of particles obtained from 4003A.D-infected cells is reduced by approximately 50% compared with yields from wild-type-infected cells (Table 3). These results are consistent with a selection for myristoyl-modified proteins occurring during capsid assembly and virion morphogenesis.

Virion assembly is initiated by P1 proteins combining to form pentameric intermediates, which subsequently assemble to form the mature virion. Cleavage of P1, generating the capsid proteins of the mature virion, is required for formation of the pentameric intermediate and subsequent assembly of the intact virion. A number of assembly intermediates have been identified in poliovirus-infected cells. These include the uncleaved capsid precursor or protomer (P1), the cleaved protomer or monomer (VP0-VP3-VP1) (5S), the pentamer (14S), the empty particle (80S), and the RNA-containing mature virus (150S) (28). To identify when myristoyl modification is critical during capsid formation, these assembly intermediates were isolated from infected cells on sucrose density gradients, and the relative incorporation of [^{3}H]myristate in VP0 was determined (Table 2). The myristoyl levels in the pentamer are between those observed for the whole-cell lysate and the mature virion, suggesting that myristoyl-modified protomers are preferentially utilized to form stable pentamers. This is consistent with an apparent decrease in myristoyl-modified VP0 capsid proteins in the protomer pool. Thus, although the nonmyristoylated protomers can be incorporated into pentamer intermediates, there is a strong enrichment at the pentamer stage for myristoyl-modified proteins. However, formation of mature virions with only myristoyl-modified protomer subunits indicates that there is an additional selection for myristoyl-modified assembly intermediates. The observation that empty capsids are not fully myristoyl modified indicates that pentamers containing unmodified protomers can assemble to form empty capsids. However, myristoylation levels in the empty capsid are reproducibly lower than that measured for pentamer intermediates, indicating that empty capsids containing pentamers with unmodified protomers appear to accumulate. Thus, selection against unmodified assembly intermediates during formation of the mature virus particle appears to occur late in virion assembly; unmodified protomers are excluded during the final stages of virus formation, i.e., RNA encapsidation and cleavage of VP0 to VP2 and VP4.

Pulse-chase experiments examined the role of this modification in the kinetics of capsid assembly. Mutant- and wild-type-infected cells were labeled at 3 h p.i. with [^{35}S]methionine. After 1 h of labeling, cells were incubated in nonradioactive medium, and maturation of the labeled assembly intermediates into mature virus particles was measured at 5 and 6 h p.i. in sucrose gradients (Fig. 4). Because overall recovery of ^{35}S label from these gradients was identical at each time point for the wild-type and mutant capsid intermediates, it is

TABLE 2. Levels of [^{3}H]myristate incorporation in 4003A and 4003A.D assembly intermediates[a]

Assembly intermediate	[^{3}H]myristate incorporation in:			
	4003A		4003A.D	
	^{3}H/^{35}S (cpm)[b]	^{3}H/^{35}S ratio	^{3}H/^{35}S (cpm)	^{3}H/^{35}S ratio
Lysate VP0[c]	596 ± 15/866 ± 15	0.69 ± 0.03	321 ± 17/1,359 ± 12	0.24 ± 0.01
Monomer VP0 (5S)	553 ± 15/718 ± 10	0.77 ± 0.03	126 ± 3/753 ± 19	0.17 ± 0.01
Pentamer VP0 (14S)	891 ± 28/1,121 ± 15	0.79 ± 0.02	480 ± 19/1,057 ± 20	0.45 ± 0.02
Empty VP0 (80S)	1,172 ± 26/1,550 ± 46	0.76 ± 0.02	632 ± 30/1,856 ± 42	0.34 ± 0.02
Mature VP0 (150S)	532 ± 12/690 ± 9	0.77 ± 0.02	583 ± 11/747 ± 5	0.78 ± 0.01
Mature VP4 (150S)[d]	21,334 ± 473/4,932 ± 58	4.33 ± 0.07	21,760 ± 227/5,054 ± 139	4.31 ± 0.08

[a] Infected-cell extracts from double-labeling experiments were analyzed in sucrose density gradients, and assembly intermediates were separated according to their sedimentation rates (in parentheses).
[b] Counts per minute (mean ± standard deviation) for each isotope in each protein band after correction for background, differential counting efficiency, and spillover between the counting channels. Means and standard deviations were calculated from counts per minute obtained from several (more than three) determinations of 10 min each.
[c] Crude lysate before analysis in sucrose gradient.
[d] Differences in ^{3}H/^{35}S ratios between VP4 and VP0 reflect the different numbers of methionine residues present in the proteins (one in VP4 and seven in VP0).

TABLE 3. Yield and infectivity of purified 4003 mature viral particles[a]

Viral particle	Yield[b] (10^4 particles/cell)	Infectivity (particles/PFU)
4003A	5.6	98
4003A.L	4.8	111
4003A.V	6.2	106
4003A.G	5.3	102
4003A.H	5.0	403
4003A.D	2.7	746

[a] Reported values each represent the mean of three preparations of virus. HeLa cells in suspension (4×10^8) were infected at an MOI of 10. Mature virus particles were purified in CsCl density gradients.

[b] Yield of virus was calculated from the measured optical density at 260 nm by using 9.4×10^{12} particles per optical density (260 nm) unit. Standard deviation values were within the range of ±15%.

possible to compare the relative rate of virion assembly observed in mutant- and wild-type-infected cells. After 1 h of labeling, peaks corresponding to protomers, pentamers, empty capsids, and mature virions are clearly observed in wild-type-infected cells, with label associated primarily with the 5S protomer peak (Fig. 4, panels 1 and 4). As expected, upon incubation in nonradioactive medium, there was a rapid accumulation of labeled virions as the label shifted from the protomer, pentamer, and empty-capsid peaks to the mature-virion peak and to a rapidly sedimenting fraction (Fig. 4). This rapidly sedimenting fraction contains mature-virus aggregates (data not shown). In 4003A.D mutant-infected cells, a 5S peak corresponding to the protomer is the predominant peak observed after 1 h of labeling; small peaks are observed in the pentamer and empty-capsid regions of the gradient, and no labeled virus is observed. Upon incubation in nonradioactive medium, there is a decrease in the protomer peak and notable accumulation of labeled empty capsids. Mature 4003A.D virus is formed during this chase period; however, it accumulates at a much slower rate than is observed in wild-type-infected cells (Fig. 4, panels 5 and 6). Consistently throughout the labeling and chase periods, larger amounts of protomer and empty capsids are present in mutant-infected cells than in wild-type-infected cells. Slower incorporation of protomers in 4003A.D-infected cells into pentamers induces a transient increase of labeled protomers in the monomer region of the sucrose gradients. The monomer peak decreases as mutant protomers are incorporated into pentamer; however, it remains higher than that observed in wild-type-infected cells. Amounts of labeled wild-type empty capsids decrease; in contrast, mutant empty capsids continue to accumulate during this period. No significant differences in pentamer levels were observed in wild-type- or mutant-infected cells. Accumulation of assembly intermediates is observed only in compartments that show increased levels of non-myristoyl-modified VP0. Thus, myristoylation of capsid precursors is required for efficient entry into the capsid assembly pathway, and preferential selection for myristoyl-modified protomers occurs at at least two stages in this pathway: during formation of the stable pentamer and during RNA encapsidation and formation of the mature virion.

The 4003A.D microplaque phenotypes (Fig. 2) could be explained potentially by partial myristoylation and the slow formation of viral particles, which lead to a reduced yield of viral particles per cell. However, because myristoylation levels in 4003A.H mutant-infected cell lysates and mature virus particles are normal (data not shown), similar explanations would not account for the small-plaque phenotype of the 4003A.H mutant. Virus production was evaluated in single-step growth experiments, and the specific infectivities were determined for all 4003A mutants. As expected by their wild-type-like plaque phenotypes, all other mutants (4003A.G, 4003A.L, and 4003A.V) displayed wild-type kinetics (data not shown). The yield of particles per cell and the specific infectivities were also identical to those of wild-type virus (Table 3). Appearance of virus in both 4003A.D and 4003A.H mutant-infected cells was also similar to that in wild-type-infected cells; infectious particles were detected at 4 h p.i., and virus production reached a plateau at 6 h p.i. (Fig. 5). Consistent with the small-plaque phenotype, infectious virus yield per cell was significantly reduced; maximum yield was consistently 10- and 5-fold lower for 4003A.D and 4003A.H, respectively, than for wild type. Kinetics of RNA synthesis and protein synthesis appear normal (data not shown). In 4003A.D, the twofold reduction in particle yield due to reduced myristoylation levels is insufficient to account for the observed reduced yield of infectious virus in this mutant. Specific infectivities for purified 4003A.D and 4003A.H mutant virus particles are approximately seven- and fivefold lower, respectively, than for wild type (Table 3). Thus, the reduced yield of infectious 4003A.H and 4003A.D viruses can be explained by the reduced infectivity of the 4003A.H particle and by the reduction of both the infectivity and particle yield of the 4003A.D mutant. Because the VP4 and VP0 capsid proteins are fully myristoyl modified in both mutant viruses, this reduction in specific infectivities must be due to substitutions of the aspartic acid and histidine residues for the alanine residue. Thus, substitutions in this N-terminal region of VP4 yield pleiotropic phenotypes. In addition to affecting the kinetics of myristoyl modification by the NMT, the identity of this amino acid residue may be important during the early stages of viral infection.

DISCUSSION

Myristoyl modification is thought to be catalyzed by the host NMT. Thus, the modification levels of the VP4003A mutants provide information on the in vivo substrate specificity of the human NMT. The substrate sequence requirements have been extensively defined only for the yeast NMT in vitro by using synthetic hexa- and octapeptides (35–37). Similar to the yeast NMT, the human NMT will efficiently modify sequences with small hydrophobic residues adjacent to the N-terminal glycine (position 3). In addition, the nonviable phenotype of a similarly constructed poliovirus mutant with a proline substitution and the wild-type characteristics of revertants with threonine or serine substitutions at this position (22) suggest that the human NMT will similarly modify sequences with small polar residues (but not proline) at this position. Unlike the yeast NMT, the human NMT will modify substrates containing aspartic acid and histidine residues at the penultimate amino acid position. Because myristoylation is a cotranslational event and because poliovirus shuts off host protein synthesis, the reduced myristoylation levels observed in 4003A.D-infected cells are probably not due to competition between the aspartic acid mutant and other endogenous cellular-protein sequences for NMT binding but rather reflect the inherent reaction kinetics of the HeLa cell NMT. Thus the in vivo substrate specificity of the human NMT appears to be distinct from but overlapping that observed in vitro for the yeast NMT.

Analysis of myristoyl-deficient mutants in vitro had indicated that the myristoyl modification might affect proteolytic

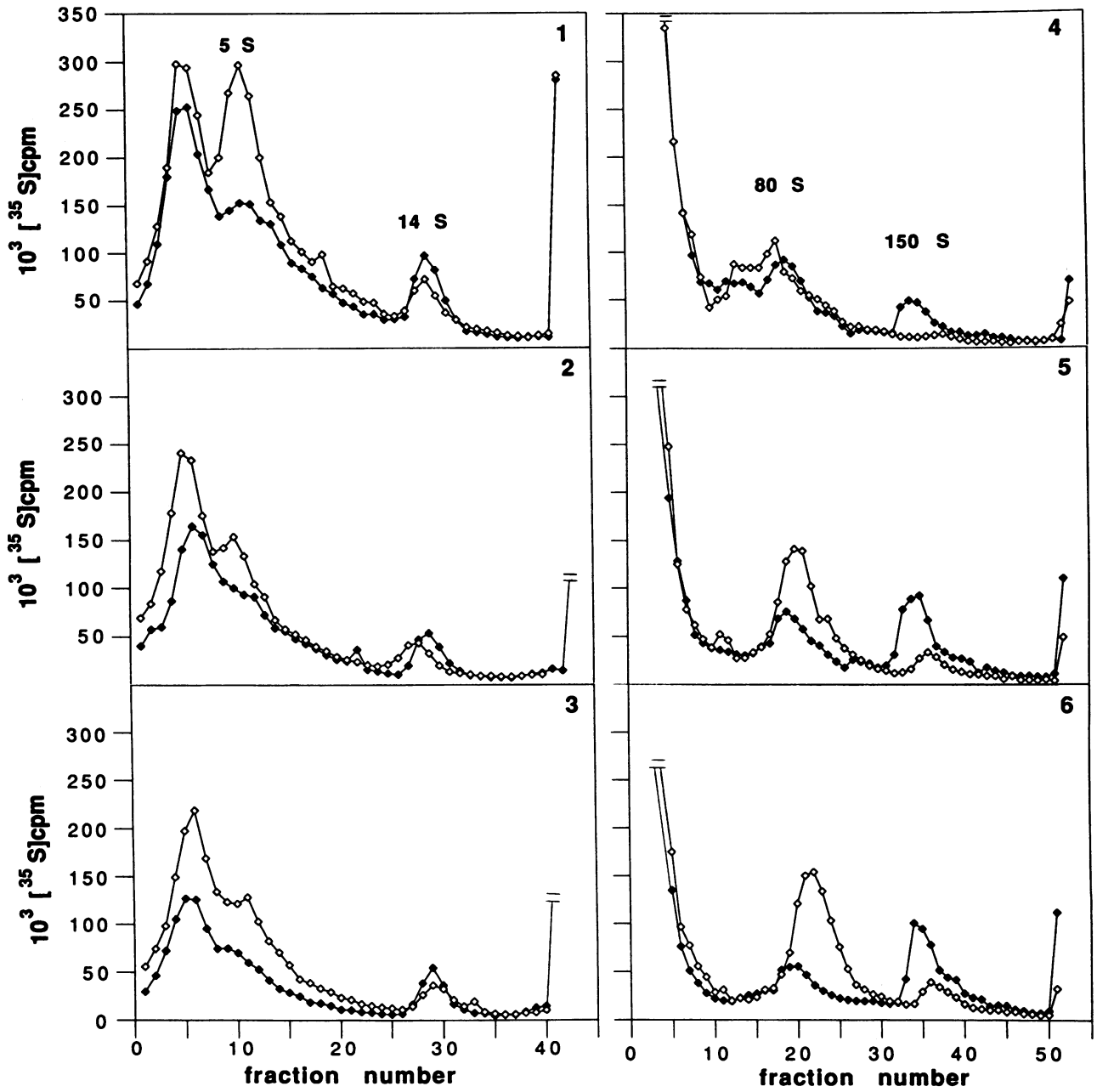

FIG. 4. Kinetics of virus maturation. HeLa cells infected with 4003A (wild type [◆]) and 4003A.D (◇) were labeled at 3 h p.i. with [^{35}S] methionine (20 μCi/ml, 1,130 Ci/mmol). At 4 h p.i., a large excess of unlabeled methionine (560 μM, final concentration) was added, and the infection was allowed to continue for another 2 h. Aliquots (10^7 cells each) were harvested at 4, 5, and 6 h p.i. Identical volumes of cell extracts were sedimented in 6 to 25% (panels 1 to 3) and 10 to 30% (panels 4 to 6) linear sucrose gradients. Sedimentation profiles of the labeled assembly intermediates at 4 (panels 1 and 4), 5 (panels 2 and 5), and 6 (panels 3 and 6) h p.i. are shown. Sedimentation rates are indicated (panels 1 and 4).

processing of the P1 precursor (18). Significant accumulation of the 1ABC intermediate (VP0-VP3), which is formed when VP1 is cleaved from P1, is observed when unmodified P1 is synthesized and processed in vitro. In contrast, proteolytic processing appears normal in cell lysates from 4003A.D- or wild-type-infected cells. There is no apparent accumulation of the 1ABC intermediate. Thus recognition of P1 by the 3CD protease and proteolytic processing of P1 to VP0-VP3-VP1 in vivo appears unaffected by the myristoyl modification.

The myristoyl-modified N termini of VP4 are located within the virus at the fivefold axis of each pentamer and are visible on the inner surface of the capsid shell (9). The five myristate hydrocarbon tails converge at each fivefold axis and then splay apart to form a cradle that appears to hold and stabilize the twisted-tube structure formed by the five VP3 N termini. Each myristoyl moiety makes three types of interactions within the mature virion: (i) it is covalently bound through an amide linkage to a specific VP4 protein; (ii) portions of its hydrocarbon chain interact with related re-

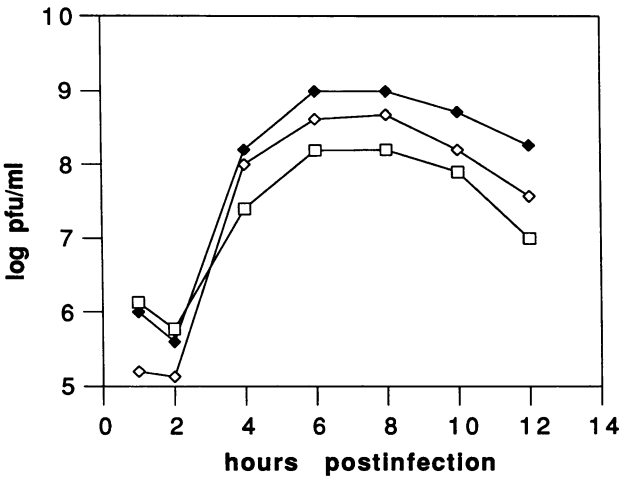

FIG. 5. Single-step growth curves for 4003A (◆), 4003A.H (◇), and 4003A.D (□). HeLa cells in suspension were infected at an MOI of 10. Total yield of infective particles at each time p.i. is expressed as $\log_{10}$ of the titer.

gions from other myristate tails at the fivefold axis; and (iii) other portions of its hydrocarbon chain interact with amino acid residues from other fivefold related VP3 and VP4 proteins. Thus the pentamer structure not only is stabilized by protein-protein interactions between protomers, but, in addition, each protomer in the pentamer structure is linked to the two adjacent protomers by interactions with the myristate tails.

Myristoylated protomers assemble into pentamers more rapidly than do unmodified protomers. Thus, myristate actively participates in pentamer formation. The nature of this participation is unclear and requires further study. If the twisted-tube structure is formed during pentamer assembly (as suggested by the structure of the empty capsid [16] and immunological characterization of pentamer and empty-capsid intermediates [27]), then the observed hydrophobic interactions in the mature virion between myristate tails and between myristate and adjacent VP3-VP4 residues may be important during pentamer formation, perhaps providing nucleation sites between monomers or stabilizing structural elements within the pentamer.

Myristoyl-modified pentamers are required for assembly stages during or after RNA encapsidation that lead to mature-virion formation. Although the mechanism for this exclusion is unknown, the woven series of myristate interactions clearly helps stabilize the pentamer structure within the mature virion. Thus an attractive hypothesis is that the myristoyl moiety is required to help maintain the pentamer subunit within the virion particle during the conformational transitions that occur in the final stages of virion maturation during and after RNA encapsidation. Alternatively, the stabilities or intracellular locations of the different intermediates may be altered by the myristoyl moiety such that only myristoyl-modified intermediates are available for RNA packaging and mature-particle formation.

It is unclear whether pentamers found in mutant-infected cells contain a mixture of modified and unmodified protomers or whether the intermediate levels measured reflect two populations of pentamers: one formed with unmodified protomers and the other formed with modified protomers. Structural arguments based on the location of the myristoyl moieties within the mature virion favor the latter interpretation. If a pentamer contained a mixture of modified and unmodified protomers, then formation of a mature virion from pentamers containing only modified protomers would require the disruption of this woven series of myristate interactions within the pentamer and would probably be energetically unfavorable. The observation that unmodified protomers of the VP4003A.P mutant can form pentamer structures (23) also supports the interpretation that the myristoyl-modified and the unmodified protomers form two distinct pentamer populations in 4003A.D-infected cells.

The reduced specific infectivities of the aspartic acid and histidine particles were unexpected. Myristoylation levels were normal for the 4003A.H mutant. In addition, the infectious particles for both mutants are fully myristoyl modified. Thus, the reduced specific infectivities indicate that the amino acid at position 4003 is important during other stages of viral infection in addition to having a role as part of the myristoylation signal. The fact that overall RNA and protein synthesis, proteolytic processing, and capsid assembly appear normal in the 4003A.H mutant (data not shown) suggests that the 4003 residue (and presumably other amino acids in the N-terminal region of VP4) is important during the initial stages of viral infection, i.e., during receptor binding and uncoating. The internal location of the 4003 residue on the inner surface of the viral capsid suggests that substitutions at this position are unlikely to directly affect virus binding to the cellular receptor. Thus it is likely that these mutants are defective in uncoating. If this is true, then the proximity of the myristoyl moiety to the 4003 residue suggests that the myristoyl modification will have an additional role(s) during the uncoating stages of infection.

Myristoylation is observed on many cellular and viral proteins (1, 4–7, 10, 14, 30, 34). In the best-studied examples, myristoylation appears necessary for correct membrane localization of the protein (17, 26, 31). Thus it has been proposed that myristoylation directs or signals membrane localization of proteins. However, several myristoyl-modified proteins appear to have no association or only transient interactions with membranes; myristoyl modification is observed on certain membrane proteins containing signal sequences, and myristoylated proteins are not segregated to a specific cellular membrane. Thus, if myristoylation is a signal for membrane targeting, the nature of this signal is highly complex. In poliovirus, the modification appears to facilitate the assembly of multimeric protein subunits; thus it appears to play a structural role in stabilizing and/or correct folding of the capsid subunits that is distinct from its potential interaction with cellular membranes. Myristoylation may perform a similar structural role in these other systems. Thus the structure of the myristoylated protein and its recognition by appropriate receptors in specific membranes rather than the presence of the myristoyl moiety per se may be the targeting mechanism. In this regard, it is interesting that a plasma membrane protein which specifically recognizes the myristoylated N-terminus sequence of $p60^{v\text{-}src}$ has been identified (25). Such structural interactions might represent elements of a more general mechanism for targeting proteins to different cellular compartments.

ACKNOWLEDGMENTS

This work was supported by Public Health Service grant AI122627 from NIH and by research grant MV-466 from the American Cancer Society.

We thank J. Hogle and J. Bodnar for their assistance and discussions.

REFERENCES

1. **Aitken, A., P. Cohen, S. Santikarn, D. H. Williams, A. G. Calder, A. Smith, and C. B. Klee.** 1982. Identification of NH2-terminal blocking group of calcineurin B as myristic acid. FEBS Lett. **150**:314–318.
2. **Bernstein, H. D., P. Sarnow, and D. Baltimore.** 1986. Genetic complementation among poliovirus mutants derived from an infectious cDNA clone. J. Virol. **60**:1040–1049.
3. **Birnboim, H. C., and J. Doly.** 1979. A rapid alkaline extraction procedure for screening recombinant plasmid DNA. Nucleic Acids Res. **7**:1513–1523.
4. **Buss, J. E., M. P. Kamps, and B. M. Sefton.** 1984. Myristic acid is attached to the transforming protein of Rous sarcoma virus during or immediately after synthesis and is present in both soluble and membrane-bound forms of the protein. Mol. Cell. Biol. **4**:2697–2704.
5. **Buss, J. E., S. M. Mumby, P. J. Casey, A. G. Gilman, and B. M. Sefton.** 1987. Myristoylated a-subunits of guanine nucleotide-binding regulatory proteins. Proc. Natl. Acad. Sci. USA **84**: 7493–7497.
6. **Buss, J. E., and B. M. Sefton.** 1985. Myristic acid, a rare fatty acid, is the lipid attached to the transforming protein of Rous sarcoma virus and its cellular homolog. J. Virol. **53**:7–12.
7. **Carr, S. A., K. Biemann, S. Shoji, D. C. Parmelee, and K. Titani.** 1982. n-Tetradecanoyl is the NH_2-terminal blocking group of the catalytic subunit of cyclic AMP-dependent protein kinase from bovine cardiac muscle. Proc. Natl. Acad. Sci. USA **79**:6128–6131.
8. **Chow, M., and D. Baltimore.** 1982. Isolated poliovirus capsid protein VP1 induces a neutralizing response in rat. Proc. Natl. Acad. Sci. USA **79**:7518–7521.
9. **Chow, M., J. F. E. Newman, D. Filman, J. M. Hogle, D. J. Rowlands, and F. Brown.** 1987. Myristylation of picornavirus capsid protein VP4 and its structural significance. Nature (London) **327**:482–486.
10. **Clark, B., and U. Desselberger.** 1988. Myristylation of rotavirus proteins. J. Gen. Virol. **69**:2681–2686.
11. **Deichaite, I., L. P. Casson, H. Ling, and M. D. Resh.** 1988. In vitro synthesis of $pp60^{v\text{-}src}$: myristylation in a cell-free system. Mol. Cell. Biol. **8**:4295–4301.
12. **Fernandez-Tomas, C. B., and D. Baltimore.** 1973. Morphogenesis of poliovirus. J. Virol. **12**:1122–1130.
13. **Guinea, R., and L. Carrasco.** 1990. Phospholipid biosynthesis and poliovirus genome replication, two coupled phenomena. EMBO J. **9**:2011–2016.
14. **Henderson, L. E., H. C. Krutzsch, and S. Oroszlan.** 1983. Myristyl amino-terminal acylation of murine retrovirus proteins: an unusual post-translational protein modification. Proc. Natl. Acad. Sci. USA **80**:339–343.
15. **Hogle, J. M., M. Chow, and D. J. Filman.** 1985. Three-dimensional structure of poliovirus at 2.9 Å resolution. Science **229**:1358–1365.
16. **Hogle, J. M., R. Syed, C. E. Fricks, J. P. Icenogle, O. Flore, and D. J. Filman.** 1990. Role of conformational transitions in poliovirus assembly and cell entry, p. 199–210. *In* M. A. Brinton and F. X. Heinz (ed.), New aspects of positive-strand RNA viruses. American Society for Microbiology, Washington, D.C.
17. **Kamps, M. P., J. E. Buss, and B. M. Sefton.** 1986. Rous sarcoma virus transforming protein lacking myristic acid phosphorylates known polypeptide substrates without inducing transformation. Cell **45**:105–112.
18. **Kräusslich, H.-G., C. Hölscher, Q. Reuer, J. Harber, and E. Wimmer.** 1990. Myristoylation of the poliovirus polyprotein is required for proteolytic processing of the capsid and for viral infectivity. J. Virol. **64**:2433–2436.
19. **Kräusslich, H.-G., and E. Wimmer.** 1988. Viral proteinases. Annu. Rev. Biochem. **57**:701–754.
20. **Kunkel, T. A.** 1985. Rapid and efficient site-specific mutagenesis without phenotypic selection. Proc. Natl. Acad. Sci. USA **82**: 488–492.
21. **Laemmli, U. K.** 1970. Cleavage of structural proteins during the assembly of the head of bacteriophage T4. Nature (London) **227**:680–685.
22. **Marc, D., G. Drugeon, A. Haenni, M. Girard, and S. van der Werf.** 1989. Role of myristoylation of poliovirus capsid protein VP4 as determined by site-directed mutagenesis of its N-terminal sequence. EMBO J. **8**:2661–2668.
23. **Marc, D., G. Masson, M. Girard, and S. van der Werf.** 1990. Lack of myristoylation of poliovirus capsid polypeptide VP0 prevents the formation of virions or results in the assembly of noninfectious virus particles. J. Virol. **64**:4099–4107.
24. **Page, G. S., A. G. Mosser, J. M. Hogle, D. J. Filman, R. R. Rueckert, and M. Chow.** 1988. Three-dimensional structure of poliovirus serotype 1 neutralizing determinants. J. Virol. **62**: 1781–1794.
25. **Resh, M. D., and H. Ling.** 1990. Identification of a 32 K plasma membrane protein that binds to the myristylated amino-terminal sequence of $p60^{v\text{-}src}$. Nature (London) **346**:84–86.
26. **Rhee, S. S., and E. Hunter.** 1987. Myristylation is required for intracellular transport but not for assembly of D-type retrovirus capsids. J. Virol. **61**:1045–1053.
27. **Rombant, B., A. Boeye, M. Ferguson, P. D. Minor, A. Mosser, and R. R. Rueckert.** 1990. Creation of an antigenic site in poliovirus type 1 by assembly of 14 S subunits. Virology **174**:305–307.
28. **Rueckert, R. R.** 1976. On the structure and morphogenesis of picornaviruses, p. 131–213. *In* H. Frankel-Conrat and R. R. Wagner (ed.), Comprehensive virology, vol. 6. Plenum Press, New York.
29. **Sanger, F., S. Nicklen, and A. R. Coulson.** 1977. DNA sequencing with chain-terminating inhibitors. Proc. Natl. Acad. Sci. USA **74**:5463–5467.
30. **Schultz, A. M., L. E. Henderson, S. Oroszlan, E. A. Garber, and H. Hanafusa.** 1985. Amino terminal myristylation of protein kinase p60src, a retroviral transforming protein. Science **227**: 427–429.
31. **Schultz, A. M., and A. Rein.** 1989. Unmyristylated Moloney murine leukemia virus $Pr65^{gag}$ is excluded from virus assembly and maturation events. J. Virol. **63**:2370–2373.
32. **Simons, J., C. Reynolds, N. Moscufo, L. Curry, and M. Chow.** 1990. Myristylation of poliovirus VP4 capsid proteins, p. 158–165. *In* M. A. Brinton and F. X. Heinz (ed.), New aspects of positive-strand RNA viruses. American Society for Microbiology, Washington, D.C.
33. **Sompayrac, L. M., and K. J. Danna.** 1981. Efficient infection of monkey cells with DNA of simian virus 40. Proc. Natl. Acad. Sci. USA **78**:7575–7578.
34. **Streuli, C., and B. E. Griffin.** 1987. Myristic acid is coupled to a structural protein of polyoma virus and SV40. Nature (London) **326**:619–622.
35. **Towler, D. A., S. P. Adams, S. R. Eubanks, D. S. Towery, E. Jackson-Machelski, L. Glaser, and J. I. Gordon.** 1987. Purification and characterization of yeast myristoyl CoA:protein N-myristoyltransferase. Proc. Natl. Acad. Sci. USA **84**:2708–2712.
36. **Towler, D. A., S. P. Adams, S. R. Eubanks, D. S. Towery, E. Jackson-Machelski, L. Glaser, and J. I. Gordon.** 1988. Myristoyl CoA:protein N-myristoyltransferase activities from rat liver and yeast possess overlapping yet distinct peptide substrate specificities. J. Biol. Chem. **263**:1784–1790.
37. **Towler, D. A., S. R. Eubanks, D. S. Towery, S. P. Adams, and L. Glaser.** 1987. Amino-terminal processing of proteins by N-myristoylation. Substrate specificity of N-myristoyl transferase. J. Biol. Chem. **262**:1030–1036.
38. **Wilcox, C., J. Hu, and E. N. Olson.** 1987. Acylation of proteins with myristic acid occurs cotranslationally. Science **238**:1275–1278.
39. **Ypma-Wong, M. F., P. G. Dewalt, V. H. Johnson, J. G. Lamb, and B. L. Semler.** 1988. Protein 3CD is the major poliovirus proteinase responsible for cleavage of the P1 capsid precursor. Virology **166**:265–270.